Optimized mounting positions for vibratory machines in buildings based on structure-borne sound power transmission and machine stability

Zhen Wang and Cheuk Ming Mak

Department of Building Services Engineering, The Hong Kong Polytechnic University, Hung Hom, Kowloon, Hong Kong

cheuk-ming.mak@polyu.edu.hk (C.M. Mak)

Dayi Ou

School of Architecture, Huaqiao University (361021), Xiamen, People's Republic of China

State Key Laboratory of Subtropical Architecture Science, South China University of Technology (510640), Guangzhou, People's Republic of China

ABSTRACT

Optimized mounting positions for isolated vibratory machines in buildings require a minimum transmission of structure-borne sound power from the machine to the floor structure and relative stability of the isolated machine. Previous work by Mak and co-investigators has indicated the importance of using structure-borne sound power to assess vibration isolation and to select the best mounting positions by considering the structure-borne sound power transmission. This paper is a first attempt to utilize both the structure-borne sound power transmission and the rotational velocity (or the stability) of the machine to select the optimized mounting positions for an isolated vibratory machine.

The results reveal that a vibratory machine should be symmetrically installed on diagonal lines of the receiving floor structure.

1. INTRODUCTION

Many vibratory machines are installed in buildings, such as chillers, boilers, pumps, air compressors, electric motors, and generators. They transmit structure-borne sound power to the floor structure. The structural acoustics process can be subdivided into four main stages: generation, transmission, propagation, and radiation. Transmission covers the transfer of oscillatory energy from the mechanisms of generation to a (passive) structure.[1] Vibration isolators are therefore used to reduce this transmission of structure-borne sound power from the vibratory machine to the floor structure. The "force transmissibility" method is widely used in the building services industry to evaluate the performance of vibration isolators.[2] The "isolation efficiency" index used in this method is based on a ratio of forces transmitted through a single contact point with and without vibration isolation. Mak and Su[3-5] indicated that the structure-borne sound power transmission is closer than the transmitted forces to the sound radiation as it considers the interaction and phase difference of motion between the complex vibratory source and the receiving floor structure. They therefore proposed the "power transmissibility" method to evaluate the performance of vibration isolation. In the development of the power transmissibility method, multiple contact structure-borne sound sources were considered. The determination of the structure-borne sound power transmission from a machine with multiple contact points to the floor structure required source activity, source mobility, and receiver mobility.[6] Mak and Su[3-5] highlighted the effect of receiver mobility on structure-

borne sound power transmission and the performance of vibration isolation. Much previous work has thus focused on receiver mobility.[7] Petersson and Plunt[8-10] proposed the effective mobility method to calculate structure-borne sound power. Gibbs and co-investigators[11, 12] proposed the reception plate method to calculate structure-borne sound power. Mayr and Gibbs[13] developed an approximation method to predict point and transfer mobility of lightweight, point-connected ribbed plates. Gibbs[14] also investigated the uncertainties resulting from utilizing a simplified method in predicting structure-borne sound power for multi-contact sources in buildings. Differences between predictions of structure-borne sound power transmission with and without terminal cross-coupling have also been investigated.[15-19]

Zu and Mak[20] proposed a method to determine the best mounting positions for a vibratory machine by considering the transmission of structure-borne sound power from the machine to the floor structure. They suggested that the best mounting positions for an isolated machine produce minimum structure-borne sound power transmission to the floor structure. In fact, source activity, source mobility, and receiver mobility not only affect the structure-borne sound power transmission, but also the stability of the machine. A relatively low structure-borne sound power transmission does not imply a relatively more stable machine or vice versa. The optimized mounting positions should therefore consider both the structure-borne sound power transmission and the stability of the isolated machine. This paper is a first attempt to utilize both the structure-borne sound power transmission and the stability of the machine to select the optimized mounting positions for an isolated vibratory machine. Yun and Mak[21] proposed using normalized average vibration velocities and rotational velocities to assess the stability of a vibratory

machine. Therefore, rotational velocity will be used in this study to assess the stability of the isolated machine with an inertia block. The mobility of the receiving floor is determined by utilizing the finite difference method. Two different boundary conditions, totally simply supported plate and totally fixed supported plate, will be used in this study.

2. THEORY

2.1. Simple Model for the Vibratory Machine and the Inertia Block

A vibratory machine model with four symmetrical contact points (p_1, p_2, p_3, and p_4) is shown in Fig. 1.

The diameter of the lower and upper parts of the machine model is D_1 and D_2, respectively. The height of both parts is H. The mass of the lower and upper parts is M_{01} and M_{02}, respectively. The mass of the vibratory machine model is M_0. It is assumed that the vibratory machine is excited by an eccentric force F_0 at the center of the vibratory machine. Take the center of the bottom face of the vibratory machine model as the coordinate origin point. The moments of inertia of the vibratory machine model throughout the coordinate origin point are given by:

$$I_{yy} = I_{xx} = M_{01}(R_1^2/4 + H^2/3) + M_{02}(R_1^2/4 + 7\times H^2/3). \quad (1)$$

The vibratory machine is symmetrically placed on an inertia block with four symmetrical contact points (q_1, q_2, q_3, and q_4) which is installed on the floor as shown in Fig. 2. The dimensions of the inertia block are $L_b \times L_b \times H_b$. The mass of the inertia block is M_b with uniform mass distribution.

Take the center of the bottom face of the inertia block as the coordinate origin point. The moments of inertia of the symmetrical vibratory machine model with inertia block throughout the coordinate origin point are given by:

$$I_{yy}^{'} = I_{xx}^{'} = I_{xx} + M_b(L_b^2 + H_b^2)/12 + I_{add} \,. \tag{2}$$

where $I_{add} = M_{01}((H_b + H)^3 - H^3)/H + M_{02}((H_b + 2H)^3 - 8H^3)/H$.

To describe the dynamic characteristics of the multi-point vibratory machine, a 4×4 source mobility matrix is expressed as follows:

$$[Y_S] = \frac{1}{j\omega(M_0 + M_b)} \begin{pmatrix} 1+\alpha^2 & 1 & 1-\alpha^2 & 1 \\ 1 & 1+\alpha^2 & 1 & 1-\alpha^2 \\ 1-\alpha^2 & 1 & 1+\alpha^2 & 1 \\ 1 & 1-\alpha^2 & 1 & 1+\alpha^2 \end{pmatrix}, \tag{3}$$

where ω denotes the angular frequency, $\alpha^2 = (M_0 + M_b) \cdot L_b^{\,2} / 4I_{xx}^{'}$.

2.2. Floor Mobility

The mobility of a plate can be determined by utilizing analytical analysis. This first solves the equation of the motion of the plate. The general two-dimensional equation of motion for a plate without excitation is given by Cremer, Heckl, and Petersson[1]:

$$D\nabla^4 v(x, y) - m^{''}\omega^2 v(x, y) = 0 \ , \tag{4}$$

where ∇^4 denotes the biharmonic operator, D denotes the bending stiffness, $m^{''}$ denotes the area density, and $v(x, y)$ denotes the velocity of the point with coordinates (x, y). The general two-dimensional equation can be solved by utilizing the variable separation method. The natural frequencies and mode shapes of a simply supported rectangular plate are given by Fahy and Gardonio[22]:

$$\omega_r = \sqrt{D / m''}\left[\left(r_1\pi / l_x\right)^2 + \left(r_2\pi / l_y\right)^2\right], \tag{5}$$

$$\phi_r(x, y) = 2\sin(r_1\pi x / l_x)\sin(r_2\pi y / l_y), \tag{6}$$

where r_1 and r_2 are the modal indices of the r^{th} mode, and l_x and l_y denote the length and width of the plate.

The general expression of the mobility of the point with coordinates (x, y) on the plate can be expressed as follows:

$$Y_r(x, y \mid x, y) = j\omega\sum_{r=1}^{\infty}\frac{\phi_r^2(x, y)}{M_p\left[\omega_r^2(1+ j\eta) - w^2\right]}, \tag{7}$$

where M_p denotes the mass of the plate and η denotes the loss factor of the plate.

The general expression of the transfer mobility on the plate between two points (x_1, y_1) and (x_2, y_2) can be expressed as follows:

$$Y_r(x_1, y_1 \mid x_2, y_2) = j\omega\sum_{r=1}^{\infty}\frac{\phi_r(x_1, y_1)\phi_r(x_2, y_2)}{M_p\left[\omega_r^2(1+ j\eta) - w^2\right]}. \tag{8}$$

In this equation, the natural frequencies ω_r and the modal shapes $\phi_r(x, y)$ need to be solved. For totally simply supported rectangular plates, analytical solutions of natural frequencies and modal shapes can be obtained. However, analytical solutions cannot be obtained for plates with other kinds of boundary conditions and complex geometries. Numerical methods, such as finite element methods and finite difference methods should be utilized to obtain approximate results. The floor model being investigated in this study is assumed to be a flat plate with uniform thickness and density. For the assumption of uniform structure, the finite difference method is quite convenient to be applied and

relatively straightforward in understanding and application.[23] Therefore, the finite difference method was utilized in this study.

2.3. Structure-borne Sound Power and Stability

Assuming that the free velocity vector of the source with inertia block is given by:

$$\left[V_S\right] = V_0[1,1,1,1]^T . \tag{9}$$

Four spring isolators were installed between the inertia block and the receiving floor. The dynamic force transmitted from the machine to the receiving floor system at the four contact points is given by:

$$\left[F^{'}\right] = \left(\left[Y_S^{'}\right] + \left(\frac{j\omega}{K} + \frac{1}{j\omega M_k}\right)[I] + \left[Y_{rq}\right]\right)^{-1} [V_S], \tag{10}$$

where K denotes the elastic coefficient of each spring isolator, M_k denotes the mass of each spring isolator, and Y_{rq} denotes the matrix of floor mobility. The active power transmitted to the floor through the four spring isolators is given by:

$$P = \frac{1}{2}\mathrm{Re}([F^{'}]^{*\mathrm{T}}[Y_{rq}][F^{'}]) . \tag{11}$$

The vibration velocity vector of the isolated machine with inertia block is given by:

$$\left[V_q\right] = \left(\left(\frac{j\omega}{K} + \frac{1}{j\omega M_k}\right)[I] + [Y_{rq}]\right)\left[F^{'}\right]. \tag{12}$$

In this research, it is assumed that the rocking motion of the machine is small. The rotational velocity indicating the rocking motion of the isolated machine with inertia block is given by:

$$R_v = \sqrt{\left|V_{q_1} - V_{q_2}\right|^2 + \left|V_{q_3} - V_{q_4}\right|^2} / L_b . \tag{13}$$

2.4. Objective Functions

The objective functions for optimizing the mounting positions for the machine with the minimum structure-borne sound power transmission and the minimum rotational velocity can be given as: Minimize $g_1 = P$ and Minimize $g_2 = R_v$, repectively. For the multi-objective optimization problem of requiring minimum structure-borne sound power transmission and minimum rotational velocity, the simplest method is to combine these two objective functions into a weighted objective function, as:

$$\text{Minimize} \quad G = w_1 \times 10 \times \log(g_1 / P_{ref}) + w_2 \times 20 \times \log(g_2 / V_{ref}), \tag{14}$$

where w_1 and w_2 denote the weighting coefficients of the level of structure-borne sound power transmission and the level of rotational velocity, repectively, which express the relative importance of the objectives; $P_{ref} = 10^{-12}$ W and $V_{ref} = 10^{-6}$ m/s. It is obvious that when G is minimized, the optimized mounting position can be obtained.

3. ANALYSIS

The parameters for the vibratory machine are: R_1=0.25 m, R_2=0.125 m, H=0.3 m, density $\rho_1 = 7.8 \times 10^3$ kg/m^3, and mass $M_m = 5.74 \times 10^2$ kg. The parameters of the inertia block model are: L_b=0.7 m, H_b=0.2 m, density $\rho_2 = 2.8 \times 10^3$ kg/m^3, and mass $M_b = 2.74 \times 10^2$ kg. The parameters for the rectangular receiving floor are: density $\rho_3 = 2.8 \times 10^3$ kg/m^3, Young's modulus $E = 2.1 \times 10^{10}$ N/m^2, loss factor η=0.02, and Poisson's ratio μ=0.2. The dimensions for the rectangular receiving floor are: length l_x=3.5 m, width l_y=3.5 m, thickness d=0.24 m, and mass $M_f = 8.23 \times 10^3$ kg. The mass of the floor is far greater than the mass of the vibratory machine. The deformation of the floor result from the weight of

the machine model is ignored in this research. Assuming that the frequency of the excitation force is 15 Hz, the elastic coefficient of the spring isolator is K=1.88×10^6 N/m.

As plotted in Fig. 3, the rectangular receiving floor is divided into a grid of 100 equal squares. The numbers in Fig. 3 indicate the sequence number of each grid point. For symmetry, only ten cases were investigated for the symmetrical arrangement of the inertia block and the machine mounted on the receiving floor. Any other cases can find their equivalent installation effects in these ten cases. Positions 1 to 10 are the ten points selected for installation of contact point q_1 of the inertia block and the machine. Mounting points q_1, q_2, q_3, and q_4 on the receiving floor for each case are shown in Table 1.

Table 1. Mounting positions of the inertia block and the machine in difference cases

Mounting position	**1**	**2**	**3**	**4**	**5**	**6**	**7**	**8**	**9**	**10**
q_1	2	3	4	5	12	13	14	22	23	32
q_2	10	11	12	13	20	21	22	30	31	40
q_3	20	21	22	23	30	31	32	40	41	50
q_4	12	13	14	15	22	23	24	32	33	42

3.1. Determination of Floor Mobility Using the Finite Difference Method

The receiving floor was divided into a grid of 100×100 equal squares in the finite difference analysis. The modal frequencies obtained by using 50×50 meshes were compared to the solutions obtained by using 100×100 meshes. The relative errors were less than 0.1%. This means that 50×50 meshes are fine enough to obtain solutions with acceptable relative errors. Assume that the receiving floor is simply supported. To

validate the results obtained by the finite difference method, natural frequencies were compared with theoretical analysis solutions. The relative errors of natural frequencies obtained by the finite difference method compared to theoretical analysis solutions were less than 0.1% for frequencies below 2000 Hz.

3.2. Structure-borne Sound Power and Rotational Velocity

According to Eqs. (9), (10), and (11), the structure-borne sound power transmission can be calculated by the following equation:

$$P = \frac{1}{2}\mathrm{Re}\left\{ V_0^2 \begin{bmatrix} 1 \\ 1 \\ 1 \\ 1 \end{bmatrix}^T \left\{ \left(\left[Y_S^{'} \right] + \frac{j\omega}{K}[I] + \left[Y_{rq} \right] \right)^{-1} \right\}^{*T} [Y_{rq}] \left(\left[Y_S^{'} \right] + \frac{j\omega}{K}[I] + \left[Y_{rq} \right] \right) \begin{bmatrix} 1 \\ 1 \\ 1 \\ 1 \end{bmatrix} \right\}. \quad (15)$$

According to Eqs. (9), (10), (12), and (13), the vibration velocity vector of the isolated machine with inertia block is given by:

$$\left[V_q \right] = V_0 \left(\frac{j\omega}{K}[I] + [Y_{rq}] \right) \left(\left[Y_S^{'} \right] + \frac{j\omega}{K}[I] + \left[Y_{rq} \right] \right)^{-1} \begin{bmatrix} 1 \\ 1 \\ 1 \\ 1 \end{bmatrix}. \quad (16)$$

The structure-borne sound power transmitted to the receiving floor and the rotational velocity can be calculated through Eqs. (13), (15), and (16), respectively. The frequency band between 1 Hz to 1000 Hz was investigated.

It is assumed that the free velocity of the machine is 1m/s in the frequency band being analyzed. The structure-borne sound power transmission of each mounting position was then calculated and plotted in Fig. 4. According to Fig. 4, it can be found that the mounting position for the vibratory machine and the inertia block with the minimum

structure-borne sound power transmission differs throughout the frequency band. To make the results more clear, for each frequency, the mounting position with the minimum structure-borne sound power transmission was picked out and plotted in Fig. 5(a). For the frequency ranges increased from 1 Hz-10 Hz to 1 Hz-1000 Hz (the increment is 10 Hz), the possibility of each mounting position to be the position with the minimum structure-borne sound power transmission was calculated and plotted in Fig. 5(b). Refer to Fig. 5(a) and Fig. 5(b), it can be observed that the mounting positions 2, 3, 6, and 8 have such small possibilities to be the position with the minimum structure-borne sound power transmission. Meanwhile, the mounting positions 1, 5, and 10 are the positions with the largest possibility to be the position with the minimum structure-borne sound power transmission, especially for the frequency band between 1 Hz and 500 Hz. With the increasing of the frequency range being considered between 1 Hz and 500 Hz, the possibility of the mounting position 1 decreased, while the possibility of mounting positions 5 and 10 increased. With the increasing of the frequency range being considered above 600 Hz, the possibility of the mounting positions 1 and 10 increased, while the possibility of mounting position 5 decreased. The mounting positions 1, 5, and 10 are symmetrical through the diagonal line of the receiving floor. It seems that the optimized mounting positions for a vibratory machine, based on the structure-borne sound power transmission, are symmetrical about the diagonal line of the receiving floor.

The rotational velocity of the vibratory machine with the inertia block for different mounting positions is calculated and plotted in Fig. 6. According to Fig. 6, the curves of rotational velocity are quite complex. Some drop and rise sharply at very narrow frequency band ranges. For each frequency, the mounting position with the minimum

rotational velocity was picked out and plotted in Fig. 7(a). For each frequency range increased from 1 Hz-10 Hz to 1 Hz-1000 Hz (the increment is 10 Hz), the possibility of each mounting position to be the position with the minimum rotational velocity was calculated and plotted in Fig. 7(b). Refer to Fig. 7(a) and Fig. 7(b), it can be observed that the mounting positions 1, 2, 3, 6, 7 and 9 have very small possibility (less than 5%) to be the mounting position with the minimum rotational velocity. While, the mounting positions 5, 8 and 10 are the positions with the largest possibility to be the mounting position with the minimum rotational velocity. The mounting positions 5, 8 and 10 are symmetrical through the diagonal line of the receiving floor. It seems that the optimized mounting positions for a vibratory machine, based on the criteria of the minimum rotational velocity, are symmetrical about the diagonal line of the receiving floor.

By comparing Fig. 5 with Fig. 7, one can see that minimum rotational velocity (that is, a relatively stable machine) does not imply minimum transmission of structure-borne sound power from the machine to the floor or vice versa. To make it more clear, the correlation between rotational velocity and structure-borne sound power transmission was considered. For each frequency, we sorted different mounting positions by structure-borne sound power transmission value and rotational velocity value in descending order, respectively. For each frequency, the correlation coefficient of rank order between these two kinds of criteria was then calculated and plotted in Fig. 8. Refer to Fig. 8, it can be found that less structure-borne sound power transmission was not strongly associated with smaller rotational velocity. All these phenomena indicate that optimized mounting positions for an isolated vibratory machine are determined by both structure-borne sound power transmission and the rotational velocity (or stability) of the machine as minimum

structure-borne sound power transmission does not imply a stable machine (low rotational velocity) or vice versa.

The receiving floor with totally fixed boundary conditions is also analyzed in this study. The structure-borne sound power transmission and rotational velocity of the symmetrical vibratory machine model at frequencies between 1 Hz and 1000 Hz were analyzed. The structure-borne sound power transmission of the vibratory machine at each mounting position is shown in Fig. 9. For the case with totally fixed boundary conditions, the mounting position with the minimum structure-borne sound power transmission for each frequency was picked out and plotted in Fig. 10(a). For the frequency range increased from 1 Hz-10 Hz to 1 Hz-1000 Hz (the increment is 10 Hz), the possibility of each mounting position to be the position with the minimum structure-borne sound power transmission was calculated and plotted in Fig. 10(b). Refer to Fig. 10(a) and Fig. 10(b), it can be observed that the mounting positions 1, 5, 8, and 10 are the positions with the largest possibility to be the position with the minimum structure-borne sound power transmission. Just like the case with totally simply supported conditions, these mounting positions are symmetrical through the diagonal line of the receiving floor.

The rotational velocity of the vibratory machine with the inertia block for different mounting positions is calculated and plotted in Fig. 11. For each frequency, the mounting position with the minimum rotational velocity was picked out and plotted in Fig. 12(a). For each frequency range increased from 1 Hz-10 Hz to 1 Hz-1000 Hz (the increment is 10 Hz), the possibility of each mounting position to be the position with the minimum rotational velocity was calculated and plotted in Fig. 12(b). Refer to Fig. 12(a) and Fig. 12(b), it can be observed that the mounting positions 1, 7, 8 and 10 are the position with

the largest possibility to be the mounting position with the minimum rotational velocity. The mounting positions 1, 8, and 10 are symmetrical through the diagonal line of the receiving floor.

The curves in Fig. 9 present some minor differences from the curves in Fig. 4, but they have the same rule almost. The mounting positions of the inertia block and the machine with the minimum structure-borne sound power transmission are on diagonal lines of the receiving floor. It can be seen that the curves in Fig. 6 and Fig. 11 have similar trends and position 10 seems to be the optimized choice because the normalized rotational velocity is small (that is, the machine is relatively stable). The analyzed results reveal that the structure-borne sound power transmission from the machine to the floor and the stability of the machine are not significantly different for the receiving floor with totally fixed boundary conditions and the receiving floor with totally simple boundary conditions. It can be concluded that the optimized mounting positions for an isolated vibratory machine with minimum structure-borne sound power transmission and rotational velocity are on the diagonal lines of the receiving floor.

3.3. Multi-objective Optimization

According to Eq. (14), the optimized mounting position of the symmetrical machine model meet the targets can be found. The two weighting coefficients w_1 and w_2 can be decided by the users in real cases. If the structure-borne sound power transmission was concerned more, the weighted coefficient w_1 should be larger; if the stability was

concerned more, the weighting coefficient w_2 should be larger. In this research, w_1 =1 and w_2 =0.5.

For the case of simply supported boundary condition, the values of *G* and the optimum mounting positions for the symmetrical machine model and the inertial block were shown in Fig. 13(a) and Fig. 13(b), respectively. Refer to Fig. 13(a) and Fig. 13(b), it can be observed that the mounting positions 1, 5, 8, and 10 are the positions with the largest possibility to be the optimum mounting position. The mounting positions 1, 5, 8, and 10 are symmetrical through the diagonal line of the receiving floor.

For the case of fixed boundary condition, the values of *G* and the optimum mounting positions for the symmetrical machine model and the inertial block were shown in Fig. 14(a) and Fig. 14(b), respectively. Refer to Fig. 14(a) and Fig. 14(b), it can be observed that the mounting positions 1, 8, and 10 are the positions with the largest possibility to be the optimum mounting position. The mounting positions 1, 8, and 10 are symmetrical through the diagonal line of the receiving floor.

4. CONCLUSION

A symmetrical machine model with an inertia block have been used to study the structure-borne sound power transmission from the machine to the floor and the rotational velocity of the machine. Two different boundary conditions, totally simply supported plate and the totally fixed supported plate, have been used. To calculate the structure-borne sound power transmission and the rotational velocity for a totally fixed supported plate, the mobility of the receiving floor system was obtained using the finite difference method. This is a first attempt to utilize both the structure-borne sound power

transmission and the rotational velocity (or the stability) of the machine to select the optimized mounting positions for an isolated vibratory machine. The results reveal that, for optimized mounting positions, the vibratory machine should be symmetrically installed on diagonal lines of the receiving floor structure.

ACKNOWLEDGEMENTS

The authors would like to thank the financial support of the Hong Kong Polytechnic University. This work was also supported by National Natural Science Foundation of China (51578252) and State Key Lab of Subtropical Building Science, South China University of Technology (2016ZB06).

REFERENCES

[1] Cremer, L., Heckl, M. and Petersson, B. A. T. *Structure-borne sound: structural vibrations and sound radiation at audio frequencies*, Springer Science & Business Media, Berlin, (2005). http://dx.doi.org/10.1007/b137728

[2] Crocker, M. J. *Handbook of Acoustics*, John Wiley & Sons, New York, (1998). http://dx.doi.org/10.1002/9780470172513

[3] Mak, C. M. and Su, J. X. A study of the effect of floor mobility on isolation efficiency of vibration isolators, *Journal of Low Frequency Noise Vibration and Active Control*, **20**(1),1-13, (2001). http://dx.doi.org/10.1260/0263092011492939

[4] Mak, C. M. and Su, J. X. A power transmissibility method for assessing the performance of vibration isolation of building services equipment, *Applied Acoustics*, **63**(12), 1281-1299, (2002). http://dx.doi.org/10.1016/S0003-682X(02)00047-6

[5] Mak, C. M. and Su, J. X. A study of the effect of floor mobility on structure-borne sound power transmission, *Building and Environment*, **38**(3), 443-455, (2003). http://dx.doi.org/10.1016/S0360-1323(02)00185-3

[6] Mayr, A. R. and Gibbs, B. M. Single equivalent approximation for multiple contact structure-borne sound sources in buildings, *Acta Acustica United with Acustica*, **98**(3), 402-410, (2012). http://dx.doi.org/10.3813/AAA.918525

[7] Mak, C. M. and Wang, Z. Recent advances in building acoustics: An overview of prediction methods and their applications, *Building and Environment*, **91**, 118-126, (2015). http://dx.doi.org/10.1016/j.buildenv.2015.03.017

[8] Petersson, B. and Plunt, J. On effective mobilities in the prediction of structure-borne sound-transmission between a source structure and a receiving structure, part 1: Theoretical background and basic experimental studies, *Journal of Sound and Vibration*, **82**(4), 517-529, (1982). http://dx.doi.org/10.1016/0022-460X(82)90405-9

[9] Petersson, B and Plunt, J. On effective mobilities in the prediction of structure-borne sound-transmission between a source structure and a receiving structure, part 2: Procedures for the estimation of mobilities, *Journal of Sound and Vibration*, **82**(4), 531-540. (1982). http://dx.doi.org/10.1016/0022-460X(82)90406-0

[10] Petersson, B. An approximation for the point mobility at the intersection of 2 perpendicular plates, *Journal of Sound and Vibration*, **91**(2), 219-238, (1983). http://dx.doi.org/10.1016/0022-460X(83)90898-2

[11] Gibbs, B. M., Cookson, R. and Qi, N. Vibration activity and mobility of structure-borne sound sources by a reception plate method, *Journal of the Acoustical Society of America*, **123**(6), 4199-4209, (2008). http://dx.doi.org/10.1121/1.2904469

[12] Späh, M. M. and Gibbs, B. M. Reception plate method for characterisation of structure-borne sound sources in buildings: Assumptions and application, *Applied Acoustics*, **70**(2), 361-368, (2009). http://dx.doi.org/10.1016/j.apacoust.2008.03.001

[13] Mayr, A. R. and Gibbs, B. M. Point and transfer mobility of point-connected ribbed plates, *Journal of Sound and Vibration*, **330**(20), 4798-4812, (2011). http://dx.doi.org/10.1016/j.jsv.2011.04.017

[14] Gibbs, B. M. Uncertainties in predicting structure-borne sound power input into buildings, *Journal of the Acoustical Society of America*, **133**(5), 2678-2689, (2013). http://dx.doi.org/10.1121/1.4795773

[15] Bonhoff, H. A. and Petersson, B. A. T. The influence of cross-order terms in interface mobilities for structure-borne sound source characterization: Plate-like structures, *Journal of Sound and Vibration*, **311**(1-2), 473-484, (2008). http://dx.doi.org/10.1016/j.jsv.2007.09.016

[16] Bonhoff, H. A. and Petersson, B. A. T. The influence of cross-order terms in interface mobilities for structure-borne sound source characterization: Force-order distribution, *Journal of Sound and Vibration*, **322**(1-2), 241-254, (2009). http://dx.doi.org/10.1016/j.jsv.2008.11.030

[17] Bonhoff, H. A. and Petersson, B. A. T. The influence of cross-order terms in interface mobilities for structure-borne sound source characterization, *Journal of Sound and Vibration*, **329**(16), 3280-3303, (2010). http://dx.doi.org/10.1016/j.jsv.2010.02.020

[18] Ohlrich, M. Predicting transmission of structure-borne sound power from machines by including terminal cross-coupling, *Journal of Sound and Vibration*, **330**(21), 5058-5076, (2011). http://dx.doi.org/10.1016/j.jsv.2011.05.014

[19] Moorhouse, A. T. Simplified calculation of structure-borne sound from an active machine component on a supporting substructure, *Journal of Sound and Vibration*, **302**(1-2), 67-87, (2007). http://dx.doi.org/10.1016/j.jsv.2006.11.022

[20] Zu, F. L. and Mak, C. M. Estimation of best mounting positions for vibratory equipment in buildings, *Journal of Vibration and Control*, **17**(2), 301-310, (2011). http://dx.doi.org/10.1177/1077546309360055

[21] Yun, Y. and Mak, C. M. Assessment of the stability of isolated vibratory building services systems and the use of inertia blocks, *Building and Environment*, **45**(3), 758-765, (2010). https://doi.org/10.1016/j.buildenv.2009.08.023

[22] Fahy, F. J. and Gardonio, P. *Sound and structural vibration: radiation, transmission and response*, Academic Press, London, (2007). https://doi.org/10.1016/B978-012373633-8/50000-4

[23] Ventsel, E and Krauthammer, T. *Thin plates and shells: theory, analysis, and applications*, CRC press, New York, (2001). https://doi.org/10.1201/9780203908723

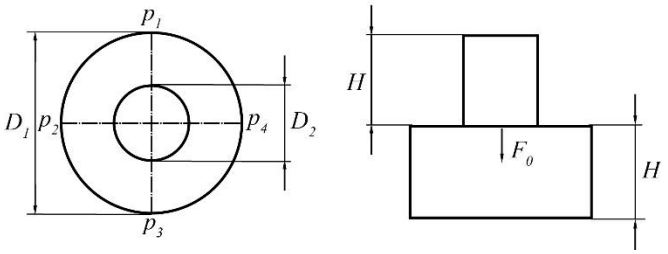

Figure 1. Schematic diagram of vibratory machine models

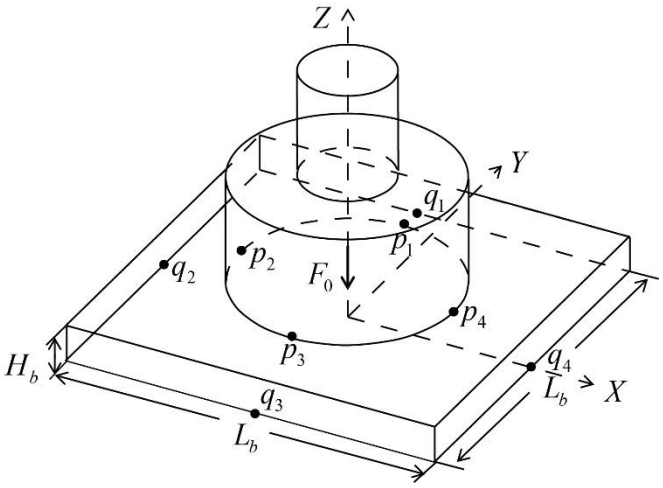

Figure 2. Schematic diagram of the vibratory machine installed on the inertia block

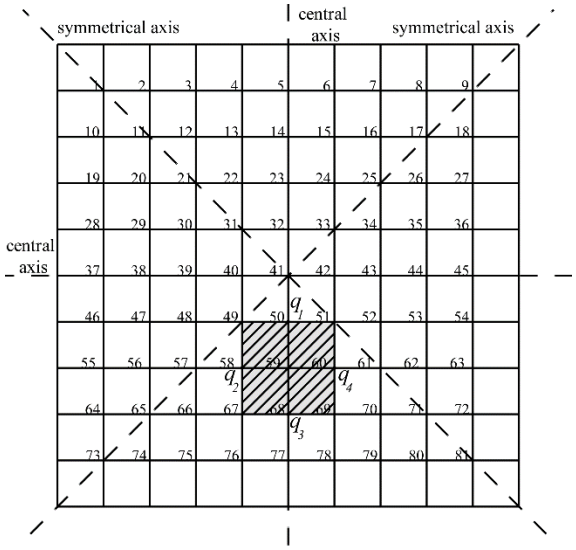

Figure 3. Schematic diagram of the floor model divided into a grid of 100 equal squares

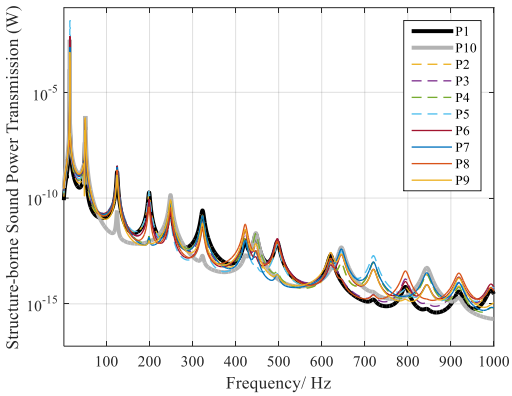

Figure 4. The sound power transmitted from the symmetrical machine model to the simply supported floor for different mounting positions

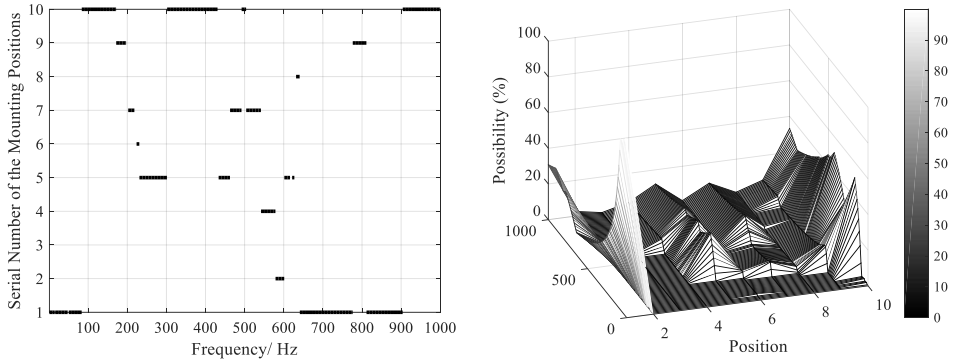

(a) (b)

Figure 5. The mounting positions with the minimum structure-borne sound power transmission: (a) the selected mounting position for each frequency (b) the possibility of each mounting position to be the one with the minimum structure-borne sound power transmission

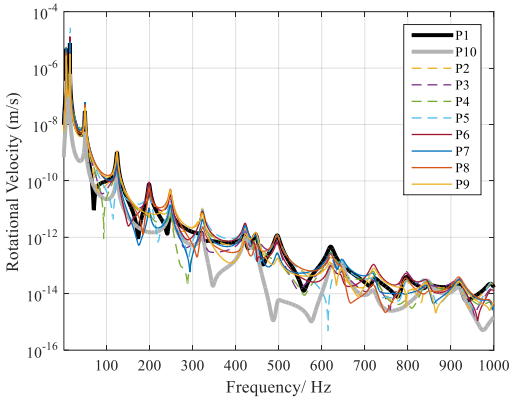

Figure 6. Rotational velocity of the symmetrical machine model and the inertial block for different mounting positions

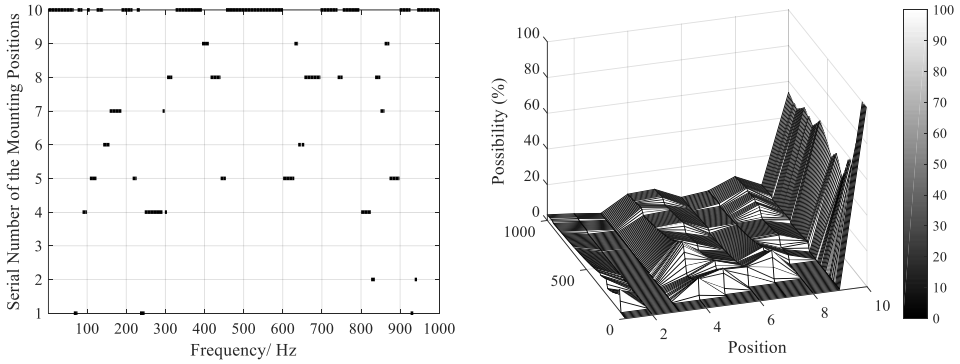

Figure 7. The mounting positions with the minimum rotational velocity: (a) the selected mounting position for each frequency (b) the possibility of each mounting position to be the one with the minimum rotational velocity

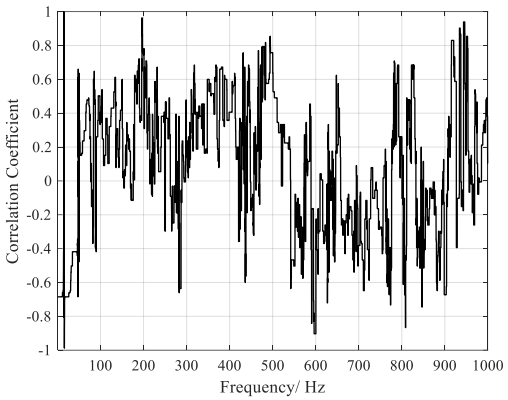

Figure 8. Correlation coefficients of rank order between structure-borne sound power transmission and rotational velocity

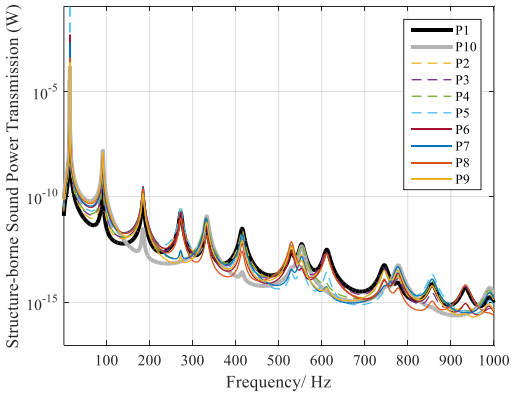

Figure 9. The structure-borne sound power transmitted from the symmetrical machine model to the fixed floor for different mounting positions

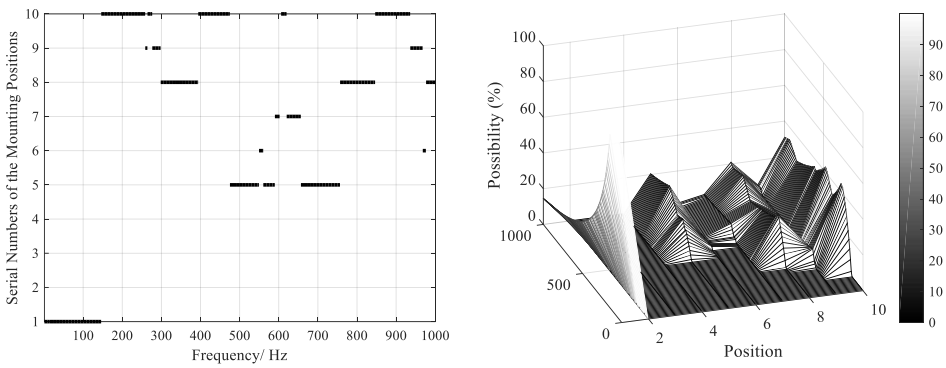

(a) (b)

Figure 10. The mounting positions with the minimum structure-borne sound power transmission: (a) the selected mounting position for each frequency (b) the possibility of each mounting position to be the one with the minimum structure-borne sound power transmission

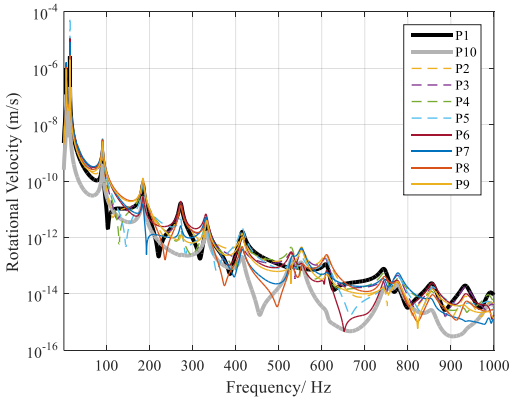

Figure 11. Rotational velocity of the symmetrical machine model and the inertial block for different mounting positions

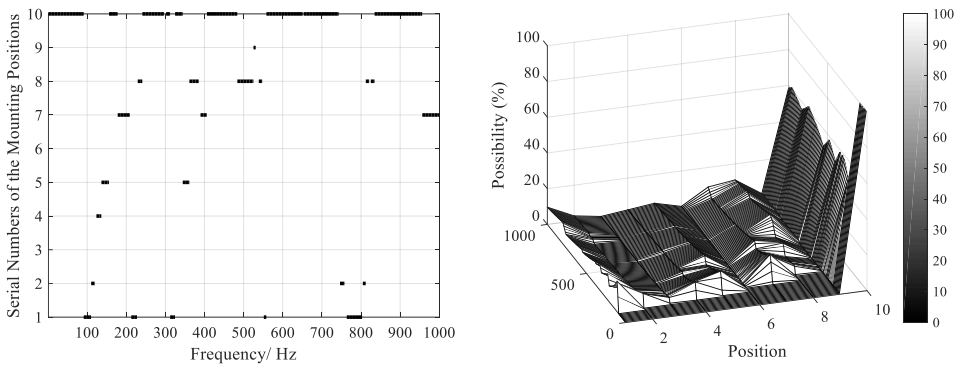

Figure 12. The mounting positions with the minimum rotational velocity: (a) the selected mounting position for each frequency (b) the possibility of each mounting position to be the one with the minimum rotational velocity

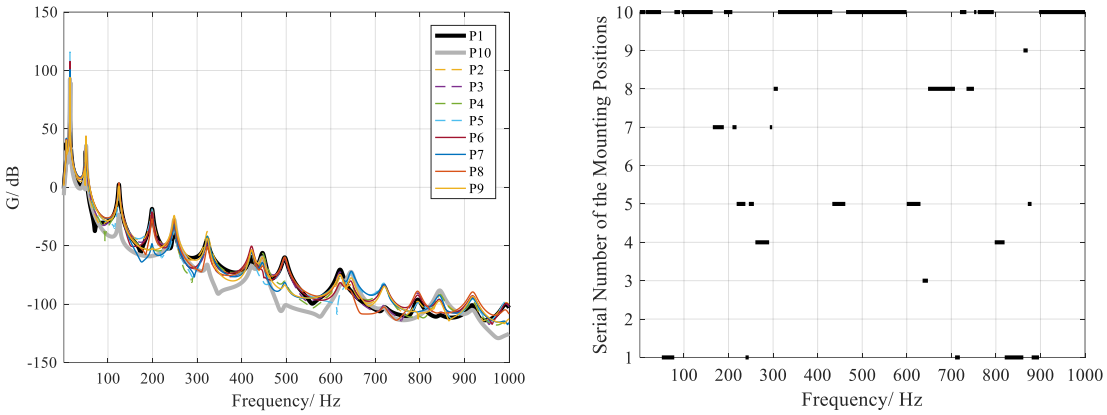

Figure 13. The floor with totally simply supported boundary condition: (a) values of the weighted objective function *G* of the symmetrical machine model and the inertial block for different mounting positions (b) the optimized mounting position for each frequency

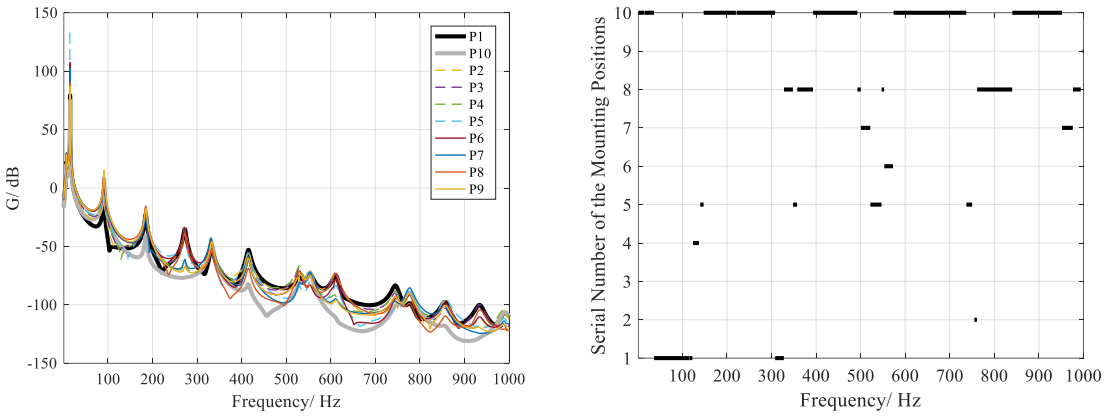

Figure 14. The floor with totally fixed boundary condition: (a) values of the weighted objective function *G* of the symmetrical machine model and the inertial block for different mounting positions (b) the optimized mounting position for each frequency